Implementation and Integration of an Experimental Vehicle Sensor Setup for Automated Parking

Ertüchtigung und Aufbau eines Versuchsträger-Sensor-Setups für automatisiertes Parken

Bearbeiter: Alberto Linares | 2288833
Betreuer: Philipp Rosenberger, M.Sc.

TECHNISCHE UNIVERSITÄT DARMSTADT

FZD FAHRZEUGTECHNIK TU DARMSTADT

Alberto Linares
Matrikelnummer: 2288833
Studiengang: Allgemeiner Maschinenbau

Bachelor-Thesis Nr. 1318-18
Thema: Implementation and Integration of an Experimental Vehicle Sensor Setup for Automated Parking

Eingereicht: September 17, 2018

Technische Universität Darmstadt
Fachgebiet Fahrzeugtechnik
Prof. Dr. rer. nat. Hermann Winner
Otto-Berndt-Straße 2
64287 Darmstadt

Erklärung zur Bachelor-Thesis

Hiermit versichere ich, Alberto Linares, die vorliegende Bachelor-Thesis gemäß § 22 Abs. 7 APB der TU Darmstadt ohne Hilfe Dritter nur mit den angegebenen Quellen und Hilfsmitteln angefertigt zu haben. Alle Stellen, die aus Quellen entnommen wurden, sind als solche kenntlich gemacht worden. Diese Arbeit hat in gleicher oder ähnlicher Form noch keiner Prüfungsbehörde vorgelegen.
Mir ist bekannt, dass im Falle eines Plagiats (§38 Abs.2 APB) ein Täuschungsversuch vorliegt, der dazu führt, dass die Arbeit mit 5,0 bewertet und damit ein Prüfungsversuch verbraucht wird. Abschlussarbeiten dürfen nur einmal wiederholt werden.
Bei der abgegebenen Thesis stimmen die schriftliche und die zur Archivierung eingereichte elektronische Fassung gemäß § 23 Abs. 7 APB überein.

Darmstadt, den 4.2.2016

(Alberto Linares)

Abstract

This thesis has been realized for the automotive engineering department of the TU-Darmstadt University. This department is currently carrying out research in the field of sensor modeling to support autonomous driving.

During this thesis the main objective is the rear sensors Bosch parkpilot URF7 implementation and integration, using the methodology described by the thesis[1]. Besides, part of the results obtained have been used for the modeling of ultrasonic sensors for valet parking use cases.

The thesis is divided in different stages. First of all, a documented bibliographic search will be carried out on the ultrasonic sensors general operation and the different most important technical specifications of an ultrasonic sensor in the field of the automotive industry as well. Among them are: the field of view, detectable objects distance ranges and accuracy of the measurement. Once the necessary information for the thesis has been obtained, the Bosch Parkpilot URF7 has been used and the different tests previously described in the methodology research have been elaborated. Besides, imparting of the initial methodology extra tests have been made based on the calculation of the distance between sensor and object in real time. It should be noted that all these tests have been run without the sensor setup installation in the car. In contrast, the position and orientation of the sensors has been fixed as in the institutes test vehicle, Honda Accord, thanks to a movable platform.

Once the system has been installed and powered with an external power supply, the basic functionality as an user level has been checked, in other words, the system calibration and the operating mode. To get a better understanding of the operation, the board that controls the Bosch sensor setup has been examined. The actual functioning of the existing hardware could not be found successfully due to the lack of information from the manufacturers. However, it is known the existence of a communication between sensors and the control unit, so that, with the realization of different tests and observing its signal with a DAQ, the signals can be read an processed. Once the operation of this Bus has been checked, the different experiments are performed to determine some technical specifications of the sensors: the field of vision (both of a sensor and of the entire sensor setup), the distance range in which a object can be detected, the operation of the cross echo and the accuracy in the measurement.

Finally, with an Arduino UNO the signal of the communication bus has been processed to obtain the distance to an object as accurate as possible in real time. In addition, the sensitivity of the results obtained with the Arduino will also be determined.

[1] Fu, J. et al.: Setup for ultrasonic models validation (2017)

Contents

List of Figures

List of Tables

1 Introduction

Nowadays there is a high interest to make cars as autonomous as possible and new technologies are helping to achieve it. The investments for developing fully autonomous cars are increasing day by day and did not reach their peak yet. With the responsibility of driving human beings, these cars have to be tested absolutely carefully. However, due to the advanced technology, testing is highly costly and time-consuming, limiting the number of testable scenarios.

Talking about parking scenarios, there are a lot of human drivers out there that can not quite handle the parallel parking job, mainly because they lack a perspective view on the object's surrounding them. It especially occurs in big cities with lots of cars and tight spaces for parking causing traffic tie-ups, vehicle damage. To help human drivers in such situations, Advanced Driver Assistance Systems (ADAS) have been developed. Systems which help you to drive, in this case, help you to park. ADAS warn you of the object proximity while you are parking with an acoustic signal. Others are more sophisticated and use cameras showing the human driver a real time picture of the car's surrounding. Latest tech systems are even able to park the car autonomously.

1.1 Motivation

The motivation of this thesis is presented as a contribution for the before mentioned problems, since together with a master thesis[2] that is running in parallel, the final objective is to validate a ultrasonic sensor model in valet parking use cases. Besides, it is colaborated for the ENABLE-S3 project in the development of simulation environments with the purpose of implementing an autonomous parking system. Therefore, all those problems that the human driver has when is parking will disappear. Besides, being able to recreate with the simulations environment infinite situations in a more efficient, cheap and fast way with the purpose of improving and checking all these systems, seeing that real environment tests are too expensive[3].

1.2 Methodology

This thesis has had a duration of 5 months in which differents methods has been followed to arrive at an objective with final results and conclusions. Note that for the collection of these results has been needed a power supply, which simulated the reverse gear feeding thus the setup. In addition, a DAQ connected to a computer, which had a Labview script implemented for the acquisition of data from the sensor setup, was needed. Remark that the chosen software was Labview due to its easy implementation with the DAQ and because it has implemented a graphical interficie that shows the information in a very visual way. To know the operation of the communication between sensor-ECU a deductive method was applied, since from the basic general knowledge of the ultrasound sensors the operation of this was deduced. Observing the signal while a object was placed at different distances and positions or even removing the object. Then, to determine the different technical specifications, a method of experimentation has been applied, in other words, some differents experiments were carried out to determine them. Finally, a method of collecting data and sampling these in real time will be realized with a microprocessor. In this case an

[2] Fu, J.: Ultrasonic sensor model (2018)
[3] Kishonti, L.: Real and simulated tests (2017)

Arduino since the university had one and Arduino is enough fast and valid for the application to be implemented.

1.3 Concretion of Assignment

The concrete assigment of this thesis is to build up a sensor setup to collect real data which will then be used to validate sensor models of ultrasonic sensors in valet parking use cases. In this thesis, URF7 Bosch autoparking pilot are the sensors studied. The first part of the thesis consists of analyzing and knowing the operation of the setup at a basic use level, apart from learning about the operation of ultrasound sensors at a general level. The second part, consists of studying the setup at a more technical level. It includes to find out the operation of the communication signal to analyze the communication between sensors and controller. With the purpose of getting real data, different experiments were performed such as obtaining the exact distance between object and sensor, determining maximum and minimum range that a sensor is able to detect an object and determining the field of view of both sensor and whole setup. Furthermore, a method was developed for starting, collecting, saving and reproducing measurement data in real time of the ultrasonic sensors. Finally, all the information and results obtained in the different experiments were documented.

2 Ultrasonic Sensors

Ultrasonic sensors are used in widely different application areas. Examples to be mentioned here are material testing, medical diagnostics, underwater sonar technology and in industrial proximity switches. Ultrasonic sensors are useful for detecting objects and measuring distances in any kind of state: gas, liquid or solid. Ultrasonic waves are used for building maps of the environment and particularly for medical diagnostics since ultrasonic waves are safer than other kind of waves that are used in hospitals. Also ultrasonic sensors are used in parking aid systems in the automotive sector. Sensors inform about the distance between the car and the objects that are around it. There are different systems that are developed together with sensors that let the driver know about an object or about what is around the car. It could be with an acoustic signal from a buzzer or in some cases with a visible signal, LEDS or LCD that show the distance from the nearest object. An ultrasound wave is defined as an acoustic wave with a frequency higher than 20kHZ, therefore it is not in the audible range of the human, since the human audible range oscillates between 20Hz-20Khz. Signals of a frequency greater than 20 kHz are called ultrasound, while those below 20 Hz are called infrasound. A 40Khz ultrasound is tipically used in air for detecting objects[4].

Ultrosound wave can be generated and detected in differents ways, but the most common technique is to use piezoelectric materials[5]. The ultrasonic sensor is based on the magnetostrictive properties of certain materials. A magnetostrictive membrane has the property of being mechanically deformed and generating ultrasound when excited by an electric current. The opposite effect also occurs, that is, a mechanical vibration producing an electric current. Therefore, these sensors emit an ultrasonic radiation that bounces off the environmental obstacles and picks up the received echoes. There are two configurations:

The first one are those that have an emitter and receiver system in the same transducer: The transducer is integrated in switched oscillating circuits, which, together with the impedance of the converter, produce optimum power conversion during transmission (serial resonant circuit) and optimum sensitivity (parallel resonance) during reception. After sending the pulse, the oscillator is turned off and the resonant circuit is switched on so that the parallel resonant frequency coincides with the emitted one. Since the membrane requires a blocking time after it sends a signal, this configuration is, in general, not sensitive to very short distances. In this blocking time, new signals can not be sent, before a signal is received or a time period expires.

Figure 1: Emitter and receiver Bosch ultrasonic sensor.

[4] Nakamura, K.: Ultrasonic applications (2012)
[5] Nakamura, K.: Ultrasonic applications (2012)

On the other hand, those that have a separate emitter and receiver system: Ultrasonic waves are generated with one of the membranes, while the other membrane is used to receive the ultrasonic waves. In this configuration, the receiving membrane is prepared to listen from the same instant in which the waves have just been emitted and therefore it is usually appropriate to measure very short distances that the configuration of a common emitter and receiver can not reach.

Figure 2: Emitter and receiver HC-SR04 sensor.

In both configurations, sensors can be affected by the cross-talking phenomenon. What it means is that the echo signal is received by another sensor or the same sensor from a previous shot if the waiting times between shots are not adequate.

Ultrasonic sensors have two sensitive detection angles, the horizontal and the vertical angles. For the automotive sector, it is interesting that the horizontal detection range is wide, while it is best if the vertical one is not wide, to avoid reflections with the ground [6]. There are also other secondary lobes in which the sensor is also somewhat sensitive, but not too much.

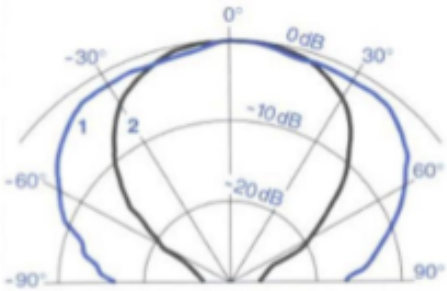

Figure 3: Vertical/Horizontal ultrasonic sensor field of view[7].

Sensors have a maximum detection distance, which depends to a large extent on the frequency of the ultrasonic wave, the sensitivity of the electronics and the membrane, and of course the transmission medium; if it is air, the wave degrades rapidly compared to aquatic environments. For the case of ultrasound in the air sensors can measure maximum distances of 3 or 4 meters.

Depending on the surface on which the signal bounces, rough or on an edge, it may be that the object is not detected, since the bounced signal would not be detected by the receiver. Normally, crystals and mirrors are theoretically detected, but their thickness may not be detected correctly. Colors do not affect this sensor.

6 Winner, H.: Handbook of Driver Assistance Systems (2014)
7 Fu, J. et al.: Setup for ultrasonic models validation (2017)

2.1 Conversion Principles

2.1.1 Piezoelectric Effect

The piezoelectric effect discovered in 1880 by Jacques and Pierre Curie is a physical phenomenon that some crystals present, due to which a difference of electric potential appears between certain faces of the crystal when it undergoes a mechanical deformation and is called direct piezoelectric effect. This effect also works in reverse. When an electric field is applied to certain faces of a crystalline formation, it experiences mechanical distortions, which is called inverse piezoelectric effect[8].

When the crystal is compressed, the ionized atoms present in the structure of each cell of formation of the crystal move, causing the electric polarization of it. Due to the regularity of the crystalline structure, and as the deformation effects of the cell occur in all the cells of the crystal body, these charges are added and an accumulation of the electric charge occurs, producing a difference of electric potential between certain faces of the crystal.

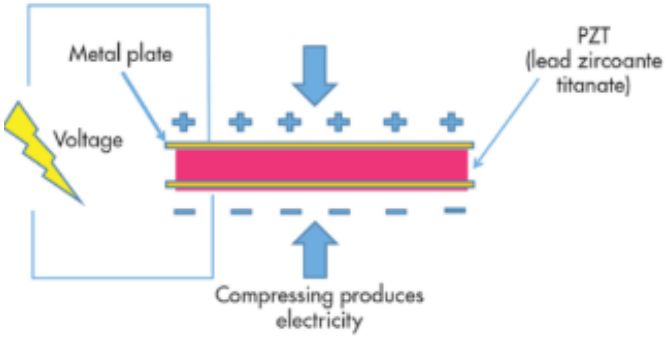

Figure 4: Piezoelectric effect[9].

On the other hand, when certain faces of the crystal are subjected to an external electric field, the ions of each cell are displaced by the electrostatic forces, producing a mechanical deformation. Since the direct and the inverse piezoelectric effect always occur together, piezo transducers can be used both for transmitting and for receiving sound.

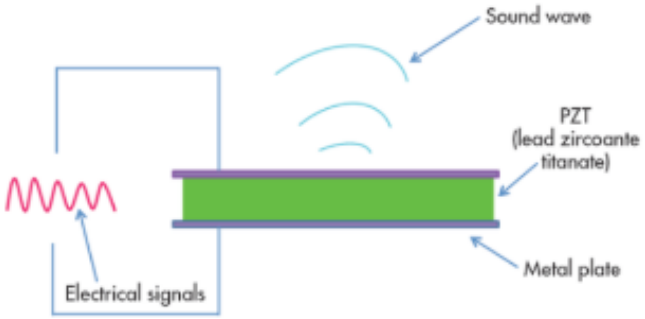

Figure 5: Inverse piezoelectric effect[10].

8 Jaffe, B.: Piezoelectric ceramics (2012)
9 Yang, C. E.: Piezo electric effect (2016)

2.1.2 Piezoelectric Material

The piezoelectric effect can only occur in non-conductive materials. In addition, all non-conductive ferroelectric materials or permanent electric dipole materials are also piezoelectric. Only quartz is used today commercially. The most important piezoelectric crystals from the practical point of view are obtained artificially.

Piezoelectric monocrystalline materials are still being developed, but the most widely used piezoelectric materials are polycrystalline ceramic materials and polymers. These materials present piezoelectric character after having been subjected to an artificial polarization. The most commonly used piezoelectric ceramic is called lead zirconate titanate (PZT)[11].

Piezoceramic materials have the property of being rigid and ductile, so they are good candidates for use as actuators, due to their large modulus of elasticity, which facilitates the mechanical coupling with the structure. In contrast, piezo-polymers are better prepared to act as sensors because they add minimal rigidity to the structure and are also easy to process. The most common way to use them is as contact sensors and acoustic transducers in the form of a thin sheet [12].

Dissymmetry in the distribution of positive and negative electrical charges sets in within the lattice of a cell below the so-called Curie temperature. This results in a permanent electric dipole moment of the single cell (Figure 6). The ferroelectricity is given from the development of domains with uniform electrical polarization that are aligned by the polarity, i.e., by a strong electrical constant field applied for a short time. The polarity is associated with a change in the length of the ceramic

The work in the field of lead-free piezoelectric ceramics has been intensive as part of the efforts not to use lead in the vehicle wherever possible. There is however no alternative to using today's ceramics that can be expected in the short term from this research.

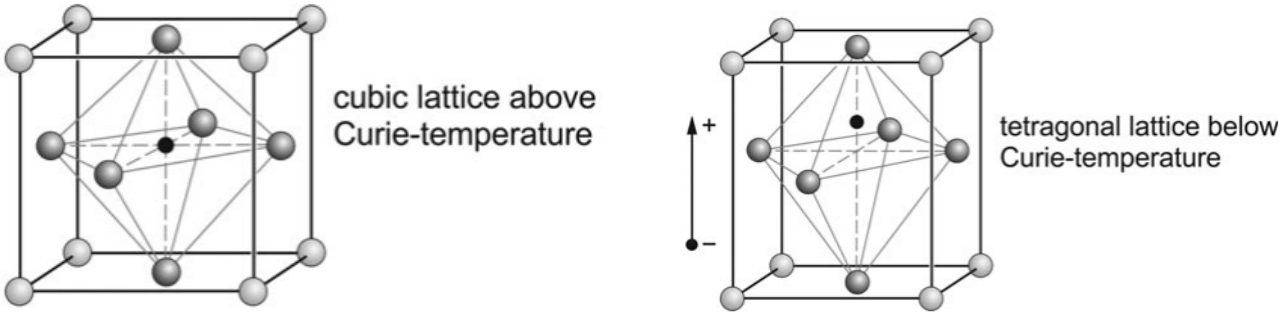

Figure 6: Titanate of lead zirconate in crystalline perovskite structure. Above and below the Curie temperature[13].

10 Yang, C. E.: Piezo electric effect (2016)
11 Nakamura, K.: Ultrasonic applications (2012)
12 Jaffe, B.: Piezoelectric ceramics (2012)
13 Winner, H.: Handbook of Driver Assistance Systems (2014)

2.2 Ultrasonic Transducer

A transducer is a device that can convert one form of energy into another, in the case of an ultrasound transducer converts electrical energy into mechanical waveform and mechanical into electrical energy, it is for this reason that most ultrasound transducers can be used to pulse echo application.

For ultrasound-based parking assist systems, a working frequency in the range of 40 to 50 kHz has proven to be the best compromise between competitive demands for good system performance (sensitivity, range, etc.) on the one hand , and high robustness against strange sounds on the other hand. Higher frequencies lead to lower echo amplitudes due to higher acoustic attenuation in the air, while for lower frequencies the proportion of noise sources in the vehicle environment increases more and more[14].

Figure 7 shows a general scheme of an ultrasound transducer in which the main parts of it can be observed, which are the following: Active or piezoelectric element, Backing and Wear Plate. The importance and functioning of them are explained below.

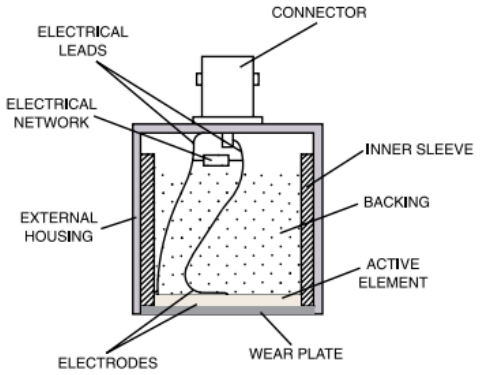

Figure 7: Different ultrasonic transducer parts[15].

2.2.1 Active Element

The active element or piezoelectric element is responsible for carrying out the electromechanical conversion previously expected, which is electrically connected to the outside through welded contacts in the electrodes that cover the piezoelectric element. Along with this element, other non-active elements are found that determine the temporary characteristics of emission and / or reception. These elements are the so-called "Backing" and wear plate. Among the different types of piezoelectric elements, piezoelectric ceramics (PZT: lead zirconate titanate) are the most commonly used due to their high conversion efficiency[16].

2.2.2 Backing and Wear Plate

These passive mechanical systems named in section 2.2 have as function to perform an emission asymmetry, which is understood as follows. The piezoelectric plate vibrates, emitting mechanical energy in both directions. The practical applications, only use the emission in only one of the faces. To this end, the

[14] Winner, H.: Handbook of Driver Assistance Systems (2014)
[15] Olympus, N.: Ultrasonic Transducers (2006)
[16] Rubio, C.: Ultrasonic transducer for automated sytems (2018)

countermass is placed on the back face, whose fundamental objective is to absorb the mechanical energy in that direction and stop the oscillation of the ceramic, originating a transducer with higher resolution.

The Wear plate on its part has two functions, protecting the active element and ensuring greater energy transfer, the latter is achieved by manufacturing it from a material with an intermediate acoustic impedance between the active element and the material on which it is expected to use the transducer[17].

2.2.3 Equivalent Circuit

A piezoceramic ultrasonic transducer can be shown close to its resonance frequency by an electrical equivalent circuit consisting of a resonant circuit in series with a parallel capacitance called $C0$, which is the disk capacitance of the piezoceramic (Figure 8). The value of $C0$ in the adhesive bonded state of the ceramic is considerably lower than before bonding in normal circumstances. Due to $C0$ has to show positive temperature dependency, this effect must be compensated by a parallel capacitance with a negative temperature dependency. In this way the resonance frequency of the electrical circuit can be kept stable with regard to the temperature.

The resonance frequency is determined by $fs = \frac{1}{2\pi\sqrt{LsCs}}$ where Ls and Cs are mechanical properties of the diaphragm.

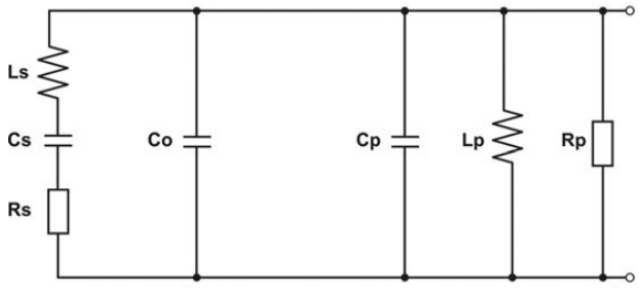

Figure 8: Transducer equivalent circuit[18].

2.3 Distance Measurements

There are different ways of generating and receiving ultrasonic waves for distance measurement applications. Commonly, continuous waves or waves in the form of a pulse can be used. There are essentially two continuous wave methods to calculate distances[19]:

1.) Based on the measurement of the phase difference between the transmitted signal and the received signal of an amplitude-modulated wave.

2.) Based on the measurement of the frequency difference between the transmitted signal and the the signal received from a frequency modulated wave.

However, most of the distance measurement applications by ultrasound are based on the time estimation that there is between the emission of a short train of pulses of ultrasonic waves, and its reception after having been reflected by some object in the environment . This period of time is commonly referred to as flight time (TOF).

17 Rubio, C.: Ultrasonic transducer for automated sytems (2018)
18 Winner, H.: Handbook of Driver Assistance Systems (2014)
19 Navarro: Ultrasonic distance measurement (2004)

2.3.1 Distances Between Pulses

Sensor generates an ultrasonic pulse which is transmitted through the medium (typically air) until it is reflected by some reflecting surface. By measuring the time between transmission and reception of the echo, the distance to the reflector can be estimated indirectly by $D = \frac{v \cdot t_f}{2}$, where v represents the speed of sound in the transmission medium and the flight time[20]:

The accuracy in the measurement of distances using this technique depends on the knowledge of v and the correct estimate of tf. The speed of sound in the air shows an almost linear dependence on temperature, which can be easily determined. Sound speed in the air is 343.2 m/s at 20ºC. Then the critical point in the measurement of distances using this technique is the determination of the time of flight. The most common way to determine flight time is by the threshold method, in which the arrival time is calculated when the echo received for the first time passes a certain level of given amplitude.

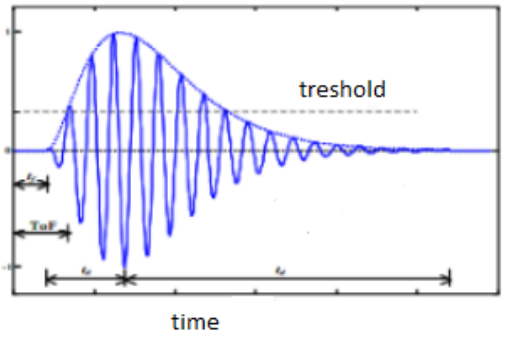

Figure 9: Ultrasound wave and its envelope wave[21].

2.3.2 Object Localization and Trilateration

Car bumper is composed by 4-6 sensors both the front and the rear one. When it is time to measure the distance from an object to the bumper, it is assumed that the objects are divided in two big groups. On one hand, there are extended obstacles, these can be, for example, a wall or a vehicle. If this is the case, then the shortest measured distance also corresponds to the actual distance. Therefore, the formula that is mentioned in the section 2.3.1 is the one that has to be used.

On the other hand, the second case is when it is a unique object. Since the distance that each sensor calculates is not the nearest from the bumper, Pythagoras theorem (1) is applied to established the distance from the object to the bumper[22].

$$D = \sqrt{DE1^2 - \frac{(d^2 + DE^2 + DE2^2)^2}{4d^2}} \tag{1}$$

[20] Carullo, A.; Parvis, M.: Ultrasonic sensor distance measurement (2001)
[21] Navarro: Ultrasonic distance measurement (2004)
[22] Winner, H.: Handbook of Driver Assistance Systems (2014)
[23] Winner, H.: Handbook of Driver Assistance Systems (2014)

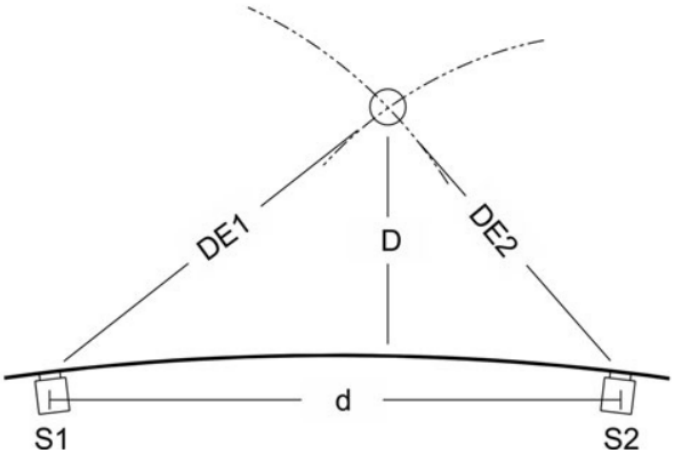

Figure 10: Trilateration obstacle distance measurement[23].

3 Bosch Parkpilot URF7

Bosch Parkpilot URF7 setup is a parking rear aid system including four ultrasonic sensor and an ECU (Electronic Control Unit). The setup warns the driver by using an acoustic signal with a buzzer and indicative LED lights, that also indicate the range of distances. In addition, it has fixing accessories to fix the sensors in the bumper and a tutorial CD.

Figure 11: Bosch Parkpilot URF7.

The four sensors of the setup are the same. Each sensor has a cable that consists of three wires which are equivalent to the three pins that each sensor has. The power pin (VCC), the ground pin (GND), and the communication pin (COMM). The COMM pin is used to establish a communication between the different sensors and the ECU. Moreover, the cables of each sensor are grouped into one and connected to the ECU. On the other hand, the buzzer and the LEDs cables are directly connected to the ECU. Also the setup has a diagnostic wire to know where the error comes from in case the system fails. Finally, the Bosch Parkpilot has the GND wire and the power wire, which is connected to the reverse gear.

3.1 Technical Specifications

The Bosch system technical specifications[24] are in the Table 1:

Table 1: Bosch Parkpilot URF7 tech specs.

Service Voltage	from 9V until 16V
Maximum Current Consumption	200mA
Service Temperature	-40° until +85°
Maximum Distance	1500 mm
Minimum Distance	300 mm
Beam Angle	No Available

3.2 System Calibration

Once the setup is mounted in a car, a calibration of the system has to be done since each car has a different bumper. The following steps are the ones that are needed to calibrate it.

1.) Place the car in front of a wall in a distance of approximately two meters.

2.) Turn on the car and set the reverse gear. Now, LED A + D are turned on (start-up mode).

3.) Drive slowly backwards in a straight line towards the wall, until the following indication can be seen: LED A + D continues to shine and, additionally, first both yellow B + C LEDs flash and then shine permanently.

4.) When the four LEDs A + B + C + D are permanently lit, stop the vehicle, set the parking brake, pull out the reverse gear and turn off the car.

5.) Turn on engine.

6.) Set the reverse gear. Now the automatic calibration procedure starts; which is indicated by the LED flashing in pairs for 45 seconds. The successful calibration is shown by the following designated sequence of LEDs: LED B + C + D + E light up.

7.) Remove the reverse gear.

8.) Move the vehicle away from the wall 2 meters approximately.

9.) Turn off engine.

10.) Cut the cable (BK = black) on the sensor wiring harness, see the Figure 12.

11.) Finally, check if the system is working properly. Turn on engine.

12.) Set the reverse gear. All LEDs flash briefly. The tone of service readiness is heard. The system is now ready for use.

[24] Bosch Operating Intructions.

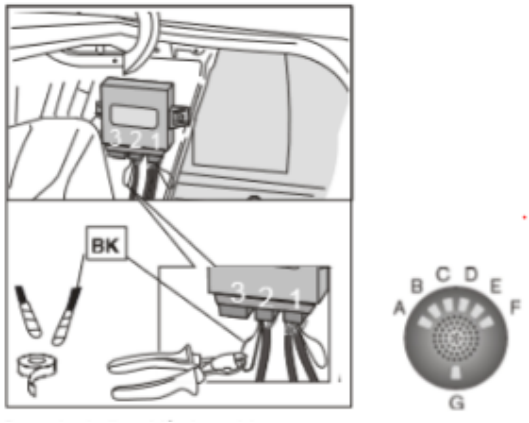

Figure 12: LEDs distribution and sensor wiring harness[25].

3.3 Bosch Parkpilot URF7 Operation

The operation of parkaid Bosch system once it is installed in the car is not complex. As the car approaches an object, the LEDs start turning on as a warning for the driver. Also, at distance of less than 700 mm between the car and the object an acoustic signal appears, which depending on the distance, will change the frequency. Distance is shown in steps of 300 mm to 100 mm thus it is not a very accurate system. The exact operation of the system is shown in Figure 13.

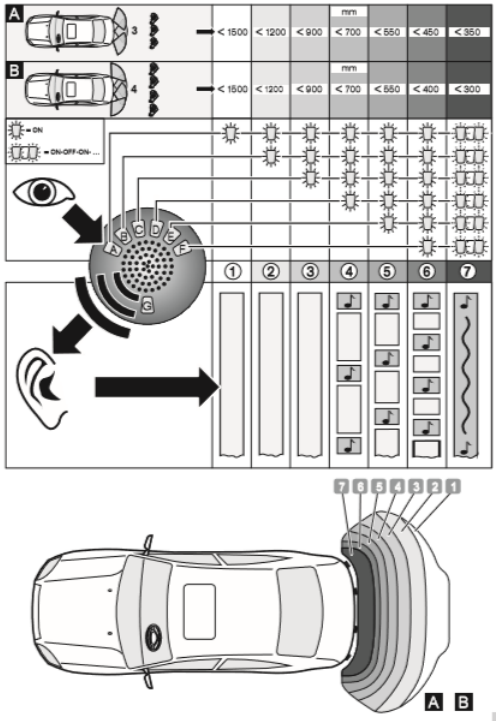

Figure 13: Bosch Parkpilot URF7 operation[26].

[25] Bosch Operating Intructions.
[26] Bosch Operating Intructions.

During the thesis different tests have been run. The data collected from these tests will be used for a parking aid simulation environment implementation. Therefore, it will be as realistic as possible. The tests can be divided into two groups: the parkaid Bosch setup technical specifications and parkaid Bosch setup data processing and data collection. Note that, for the different tests, the four sensors have been placed in the same disposal as in the workshop test car, Honda Accord. For the realization of these tests, different hardware and software instruments were needed.

The first group of tests are carried out to have a better accuracy of the Bosch setup technical specification since the one that is described by the parkaid Bosch setup itself in section 3.3 is not accurate enough. In addition, the results obtained have an effect on the environment simulation because the values should be implemented with the highest possible accuracy. First, the COMM Bus operation between the ECU and a sensor is studied. Once the COMM Bus operation is known, looking at its signal, the distance between object and sensor can be determinated. In addition, the maximum object detect distance, minimum object detect distance and field of view (FoV) have been determined. The setup to perform these experiments is shown in Figure 14.

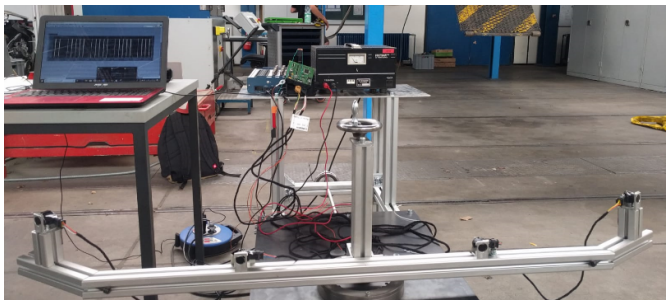

Figure 14: Final Setup for the experiments.

On the other hand the second test group consists of collecting data from each sensor COMM Bus with an Arduino. This information is processed with a script that has been developed to obtain the distance from the sensor to an object in real time. Besides, another test will be done to calculate the sensitivity of the calculated distance and thus be able to add this to the environment simulation. The setup for these experiments is shown in Figure 15.

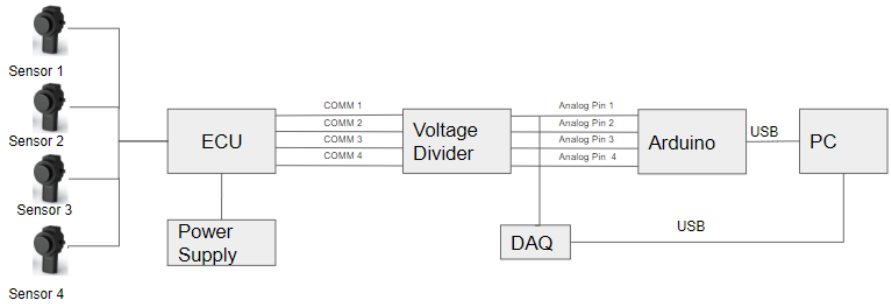

Figure 15: Experiments block diagram.

4.1 Hardware and Software

4.1.1 Power Supply

Rear park aid Bosch setup is supplied when the reverse gear is set. As the Bosch setup is outside the car, a power supply is needed. It provides a voltage of 13.8V. (Figure 16).

Figure 16: Voltcracft power supply.

4.1.2 National Instrument DAQ and Labview

Data collection is the process of detecting electrical or physical phenomena such as voltage, current, temperature, pressure or sound with a computer. A data acquisition system consists of sensors, data acquisition device and a computer with programmable software[27]. In the following tests the data collection of the electrical signal is taken with the multifunction DAQ NI USB6363 X-Series. About software, Labview has been used due to its easy synchronization with the DAQ. In addition, Labview allows to show the collected data in a more visual way thanks to its graphic interface. Therefore, a computer with Labview is needed. The software developed in Labview for the data sample is shown in Figure 17.

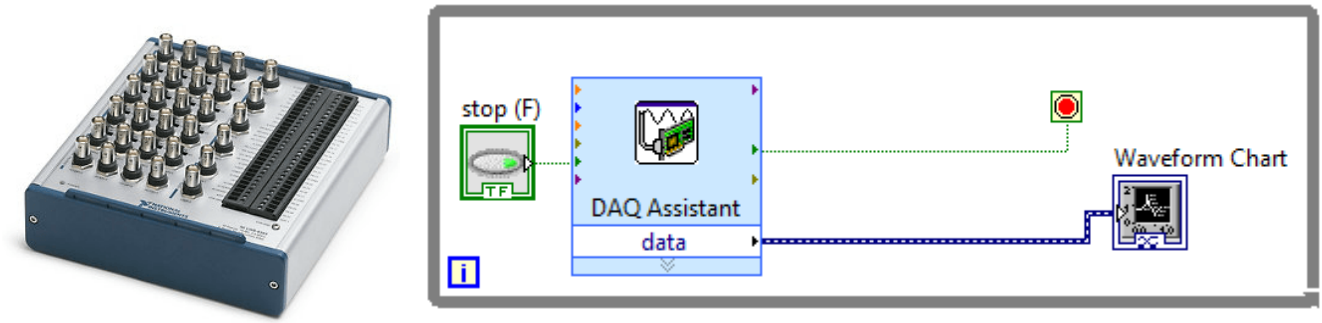

Figure 17: NI hardware and Labview softwae implemented.

[27] Data acquisition.

4.1.3 Arduino

Arduino is an open source electronic platform based on hardware and software. Arduino will be the microcontroller chosen for the tests since it has the following advantages in comparison to others:
1.) The university owns an Arduino.
2.) As an open source platform, there are many resources available on Internet.
3.) Compared to other one development boards, Arduino and related products are relatively cheap but also of excellent quality.
4.) Instructions in the Arduino software language are not complex, with basic programming knowledge one can apply Arduino quickly.
5.) The program code is loaded directly on the Arduino board through a USB cable.
6.) Its technical specifications are powerful enough for the application to be carried out.
7.) Multi platform. The Arduino programming environment is executable in Windows, Macintosh OSX and Linux[28].

The Arduino board chosen is the Arduino Uno Rev3. This consists mainly of digital and analog inputs and outputs, microcontroller and USB interface.

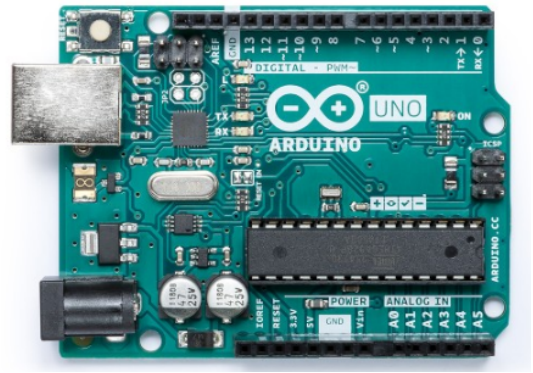

Figure 18: Arduino UNO Rev3 board[29].

Arduino UNO Rev3 technical specifications are shown in the Table 2. Note that Arduino can be powered through USB or its pins.

[28] Arduino IDE.
[29] Arduino UNO Rev3.

Table 2: Arduino UNO Rev3 technical specifications[30].

microcontroller	Atmega328P
Operating Voltage	5V
Input Voltage (recommended)	7-12V
Input Voltage (limit)	6-20V
Digital I/O Pins	14
Analog Input Pins	6
DC Current per I/O Pin	20mA
DC Current for 3.3V Pin	50mA
Flash Memory	32 KB
SRAM	2 KB
EEPROM	1 KB
Clock Speed	16 Mhz

Arduino IDE is the software that is used by default for programming with Arduino. This software uses a simplified C and C++ language, since it has different libraries included. It is based on the Processing environment as well as a programming language based on Wiring. The Arduino IDE comes with a code editor and integrates gcc as a compiler[31].

4.1.4 Static Tests Setup

A setup previously assembled by other students is used to fix the sensors position during the experiments and thus simulate the bumper of a car (Figure 19). The front bar of this setup has been modified in such a way that the sensors are located in the same position as institute's Honda Accord test car. Therefore, distances have been taken between the four rear sensors of the car and a new front bar has been designed. Note that the base can be moved small distances and the front bar can take different angles thanks to a rotating mechanism.

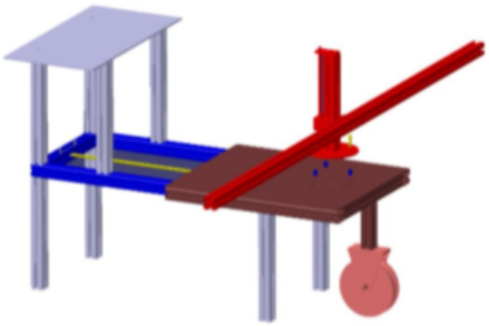

Figure 19: Previous static tests setup[32].

[31] Arduino IDE.
[32] Fu, J. et al.: Setup for ultrasonic models validation (2017)

The distance between the central sensors of the institute car is 50 cm. Whereas the distance between the central sensor and the side sensor is 41 cm. Note that, the side sensors are 7 cm higher and 5 cm behind than the middle ones. Once the distances are known a new bar is designed keeping the same distances between sensors(Figure 20).

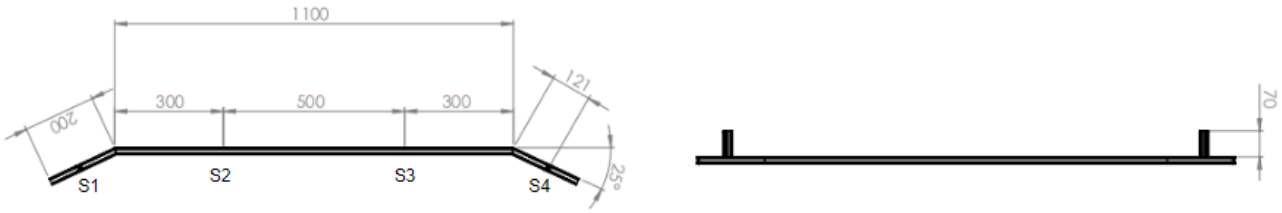

Figure 20: Layout for the setup bar.

It has been decided to apply an angle between both bars to prevent the sensors from detecting their own bar all the time. In case both were located with an angle of 90° with respect to them, sensors will detect all the time these ones.

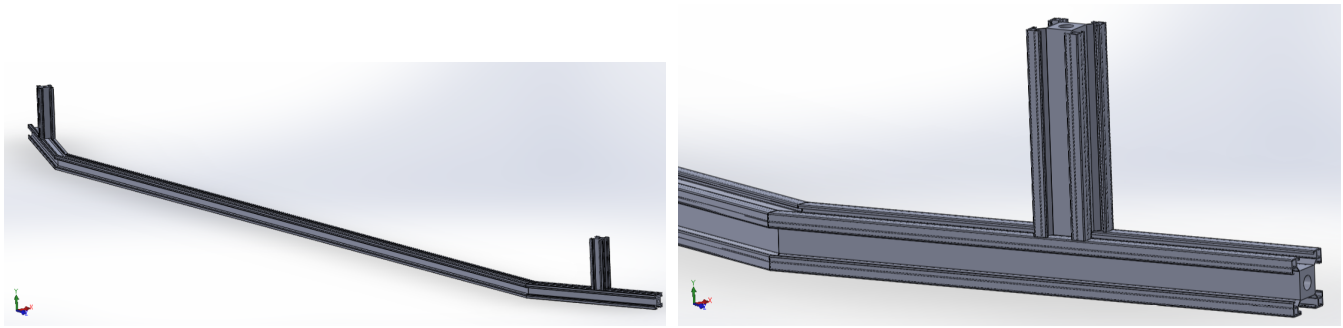

Figure 21: New setup bar.

Finally, thanks to the shape of the metal bar with the pieces that are shown in Figure 22, screws and plastic ties sensors can be fixed in the bar.

Figure 22: Fixing pieces for sensors[33].

[33] Fu, J. et al.: Setup for ultrasonic models validation (2017)

4.2 COMM Bus Operation

Once the system is powered, that is, the reverse gear is set, the sensors and ECU module are ready to work. To calculate the distance both ECU and sensors communicate through the COMM Bus. When this is initialized, large amount of data is sent by the ECU to the sensors. During this initialization ECU is responsible for assigning certain level of voltage gain to them. After this, the communication between both ECU and sensors starts. In this communication, two types of pulses can be distinguished according to their voltage. Thanks to this, it can be determined which one sensor or ECU is talking in the bus. Then, when the ECU is active on the COMM Bus, it pulls the voltage from the Bus down from 8V to 1V . While the sensor, when is active, pulls the voltage down to 1.5V. During this communication, the COMM Bus signal of one of the sensors is observed with the Labview. The ECU activates each of the sensors with a ping, then the sensor sends the ultrasound signal, which is viewed as a lower voltage pulse on the COMM Bus, to detect if there is any object. In case there is an object the sensor will receive and echo. Otherwise the sensor will wait a specific time, which is called Time of Flight(TOF), and then the same process will be repeated again.

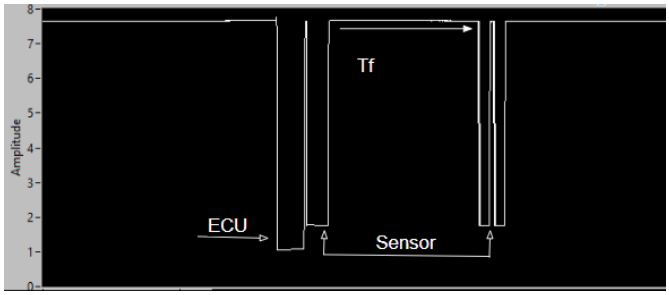

Figure 23: COMM Bus signal different pulses.

4.3 Distance Measurement Test

The objective of this test is to measure the distance from one of the set up sensors to an object. Therefore, the remaining three sensors are turned away to avoid influencing the signal of the active sensor. For this experiment, the COMM Bus data is collected and analyzed. First, the COMM Bus signal is seen when the sensor has no object to detect. In this case the signal is shown in Figure 24. The signal is periodic. In each period, four pulses are distinguished. Due to its voltage, three come from the ECU and one from the sensor. The sensor pulse is equivalent to the ultrasonic signal sent by itself to detect an object. Since there is no object, the sensor receives nothing. The pulse before the sensor is sent from the ECU to activate the sensor.

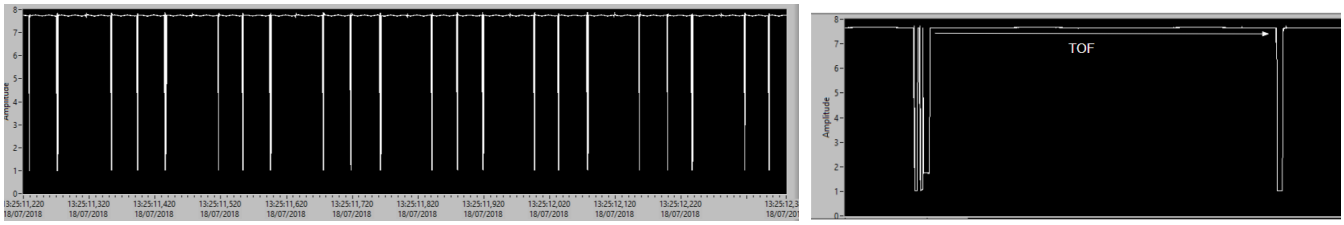

Figure 24: COMM Bus signal no object detection.

Then an object is placed in front of the sensor and the same process is repeated. The signal obtained from the COMM Bus is shown in Figure 25. Now, it is observed that after the sensor activation there are two pulses that come from the sensor. One is the pulse sent for the object detection and the other one, the pulse according to the object that has been detected.

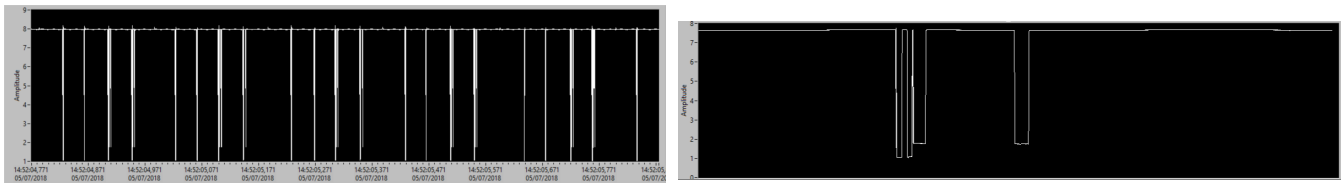

Figure 25: COMM Bus signal one object detection.

To calculate the distance from the sensor to the object, the distance in time between the two pulses, the sent and the received, is measured. Once the tf is obtained from the graph, the equation (2) in section 2.3.1 is applied and the distance is calculated[34].

$$D = \frac{v \cdot t_f}{2} \tag{2}$$

Finally, another object is placed in the field of view of the sensor to verify if the sensor is able to detect two objects at the same time. The COMM Bus signal obtained is shown in Figure 26. It is seen that two pulses are received from a single sent pulse. The distances between sent pulse and received pulse are calculated, both with the same procedure previously explained. The real distance is the same as the calculated for both cases. Therefore, the setup is able to detect two objects at the same time.

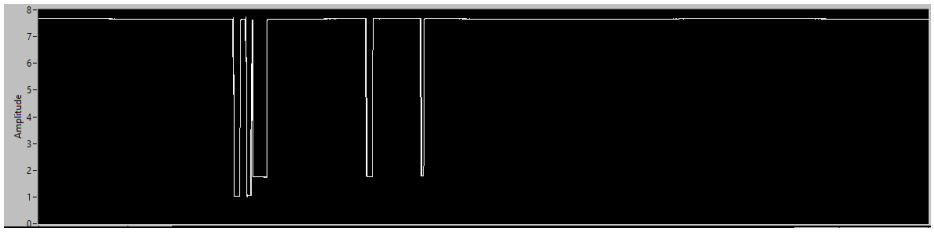

Figure 26: Two objects detected in the same period.

4.4 Maximum and Minimum Range Distance

The objective of this experiment is to determine the maximum and minimum detectable distance between a sensor and a wall. For this experiment, the setup is placed in front of a wall with enough distance between them in order that the wall can not be detected by the sensor (Figure 27). First, it is placed at 4 meters and the COMM Bus signal is viewed, the sensor does not detect anything. The setup is then brought closer to the wall in steps of 5 centimeters and the signal is observed in each step.

[34] Carullo, A.; Parvis, M.: Ultrasonic sensor distance measurement (2001)

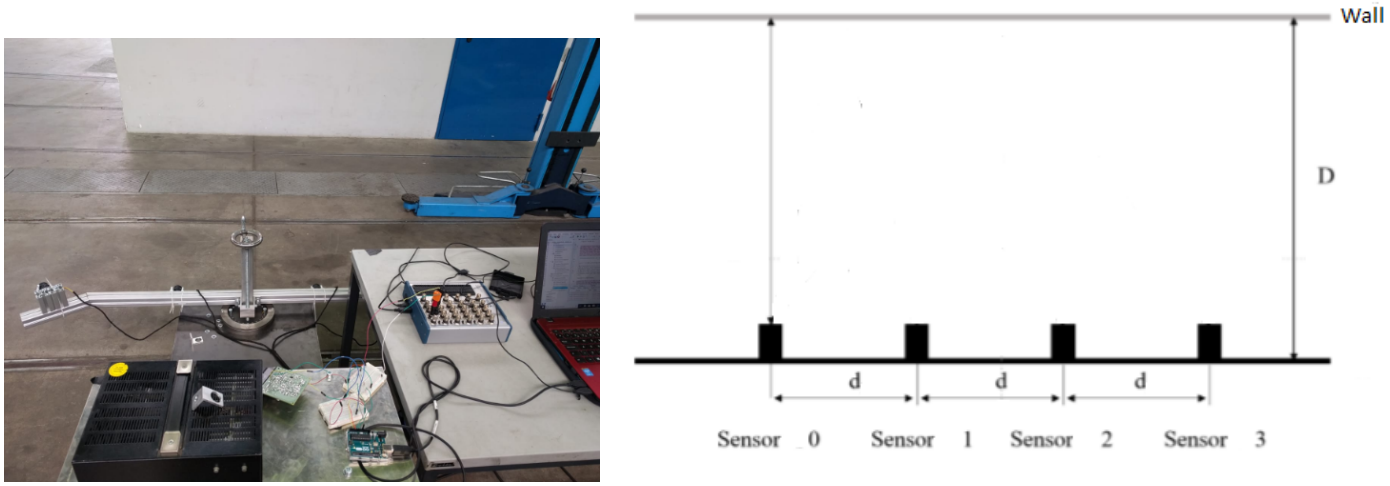

Figure 27: Wall test setup.

The following Figure 28 shows the percentage of periods detected in a total of 10 periods examined. During the different steps, it is shown how the sensor is detecting the object with greater probability until the distance is less than 3.60 meters then the sensor is always detecting the wall. For that reason, 3.60 meters is the distance that is established as the maximum distance in which the sensor can detect an object.

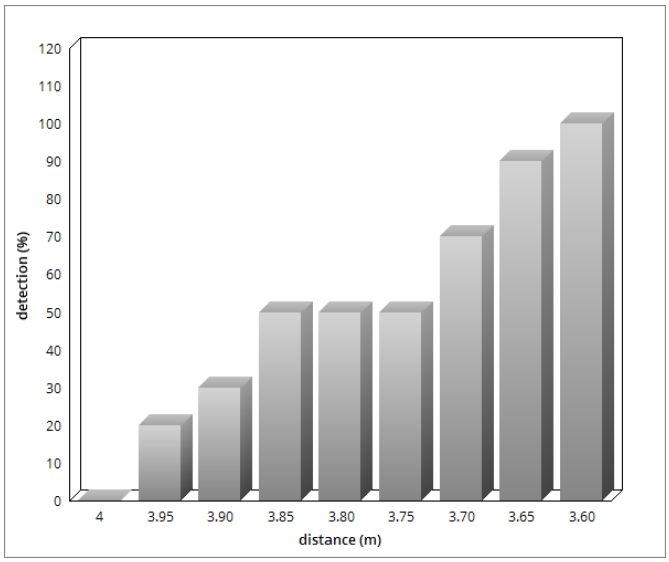

Figure 28: Object detection probability in ten periods.

On the other hand, to calculate the minimum distance an object is placed just right in front of one sensor. It is suppose to be normally a distance where the system does not detect an object, this distance could be more or less, but in this case when an object is placed just in front of the sensor, the system was all the time advertising with LEDs and acoustic signal that an object was really near. Therefore, the sensor has no detectable minimum distance.

4.5 Sensor Field of View Determination

The objective of this experiment is to determine the field of view and the cross echo operation for a sensor and for the whole parkaid Bosch setup. In the procedure of this experiment a point object is used to determine both. An object is placed at a distance d and it is moved parallel through the X axis (Figure 29)[35]. The first point at which the sensor detects the object is fixed as the limit of the sensor field of view. To fix the other side, the same procedure is repeated. To calculate the angle of this point, a trigonometric relationship is applied that is given by the following equation (3):

$$\beta = \tan^{-1}\left(\frac{x}{d}\right) \tag{3}$$

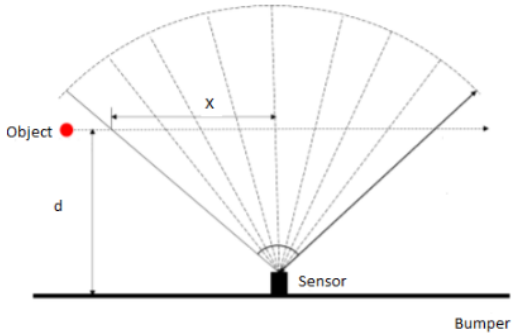

Figure 29: Field of View experiment procedure.

To determine the sensor field of view, the experiment explained before has been carried out. In this experiment the Figure 14 setup has been used and all the sensors except one have been turned away to avoid the cross-echo. The experiment has been run for two different positions of the sensor, having a difference between them of 90° (Figure 30)[36]. Therefore, both the vertical and the horizontal field of view have been determined.

Figure 30: Sensor position to determine both FoV.

[35] Fu, J. et al.: Setup for ultrasonic models validation (2017)
[36] Bosch Ultrasonic Sensor.

Different point objects have been used; a square shape metal stick, a round shape plastic tube and a round shape metal tube (Figure 31). All of them have almost the same size. Depending on the specific object used, the results obtained are different. The best result were collected with the metal stick with a square shape.Therefore, it is verified that the material of the object used for the experiment does not affect the determination of the field of view but the form affects. According to the shape of the object, the direct echo is received by the sensor better or worse (Figure 32).

Figure 31: Point objects used for the experiments.

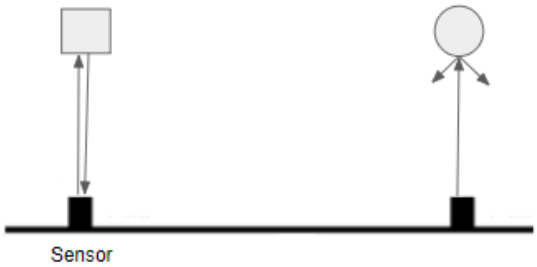

Figure 32: Echo behaviour depending on the shape.

The field of view, both horizontal and vertical, has only been determined for the left half plane, replicating the same result obtained for the right half plane, assuming that the Bosch sensor is ideal.

The measurements have been taken for different values of d. The range of d goes from 0 to 2500 mm in steps of 100 mm-200 mm. In the Table 3 below the square shape metal stick results are shown.

Table 3: FoV Bosch sensor measurements.

Horizontal FoV Measurements		Vertical FoV Measurements	
X (cm)	d (cm)	X (cm)	d (cm)
48.5	10	8	10
59	21	17	20
63	30	19.5	30
81	59	30.5	40
101.5	79	25.5	50
97.5	100	28.5	60
93	115	32	70
92.5	135	35	80
106	144	33	90
84	150	30	100
89	160	26	115
51	170	21.5	130
23	180	17	145
5	200	12.5	160
0	250	8	175
		0	185

These measures have been replicated in AutoCAD for the square shape metal stick. The both field of view horizontal and vertical are shown in the following Figure 33 and Figure 34 .

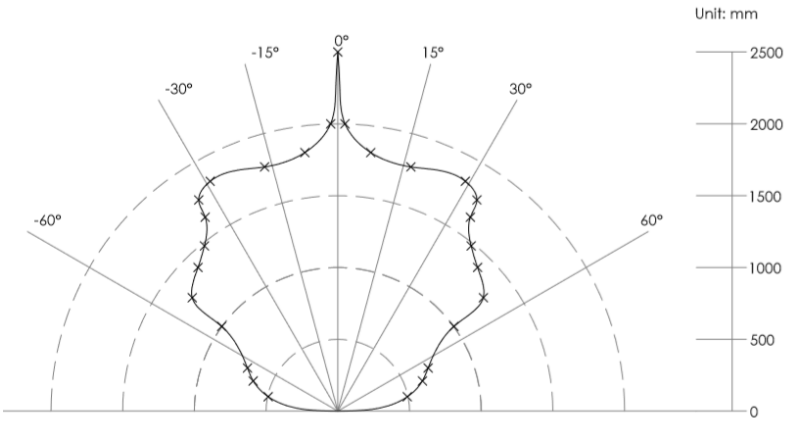

Figure 33: Bosch sensor horizontal field of view.

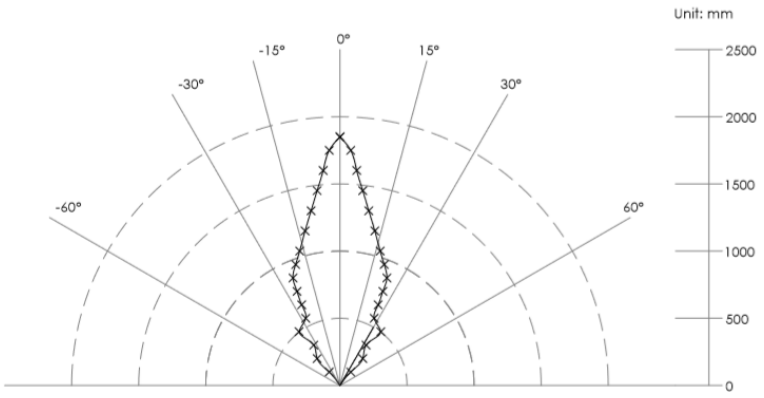

Figure 34: Bosch sensor vertical field of view.

4.5.1 Cross Echo Operation

The cross echo occurs when a sensor receives the signal bounced by an object and this signal came from another sensor.

To detect the cross echo in the COMM Bus, first an object is placed in front of one of the setup sensors, in such a way that this object is not detected by any of the other sensors in the setup. The sensor's 1,3 and 4 signal COMM Bus is watched with Labview Figure 24. Therefore, the sensors are not detecting any object, while the signal of sensor 2 shows that it detects an object (Figure 25). This first configuration is done just to compare the COMM bus signal when it is detecting a cross-echo.

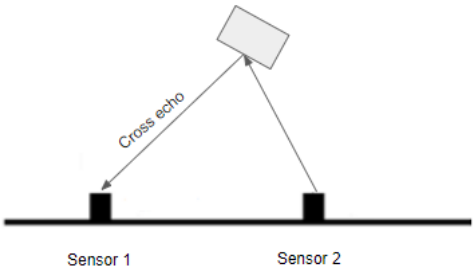

Figure 35: Cross-Echo Setup.

To facilitate the detection of a cross echo, an object is placed between sensor 1 and sensor 2 (Figure 35). While watching the COMM Bus signal of sensor 2 it can be seen that a period is formed by five pulses that come from the ECU instead of three.

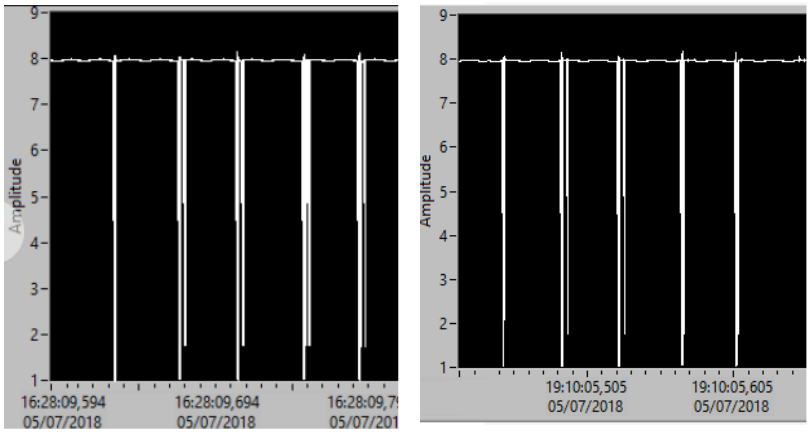

Figure 36: COMM Bus signal cross echo for different scenarios.

In the left picture of Figure 36, it is presented the COMM Bus signal of a sensor in a cross echo scenario where that sensor is receiving a cross echo from another sensor and also its own echo. It is known because after the last two large pulses it can be viewed two short pulses, the sent and its own echo whereas in the two middle large pulses it can be seen just one short pulse which is the cross echo. On the contrary on the right picture, the performing sensor is just receiving the cross echo.

4.5.2 Whole Setup Field Of View Determination

Even though the field of view of a sensor has been determined, replicating this for each of the four sensor can not be applied for the whole system field of view. Since for intermediate zones between sensors, a sensor is able to receive the cross-echo and not its own echo. Which means that for only one sensor that object would be outside of its field of view, while for the whole setup that object would be inside the field of view. Therefore, the same experiment has been repeated as in section 4.5, but with the four sensors in operation. The four communication buses were observed at the same time to know if any of the sensors was receiving its own echo or cross-echo and thus determining the limit of the field of view. This experiment has been done with the metal stick with square shape and the plastic stick with round shape. The results obtained are the following Figure 37 and Figure 38 .

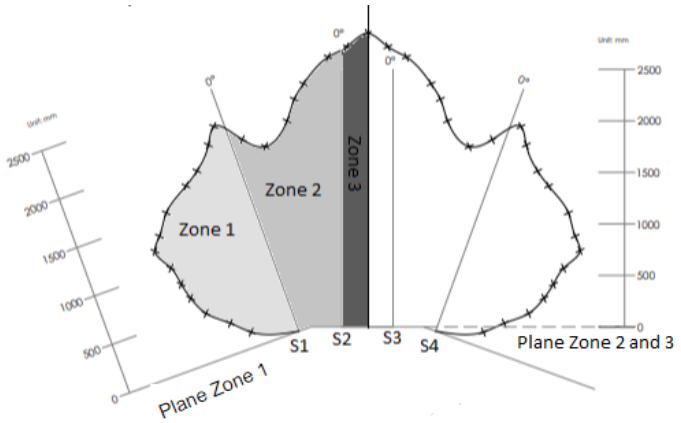

Figure 37: Whole system FoV metal stick.

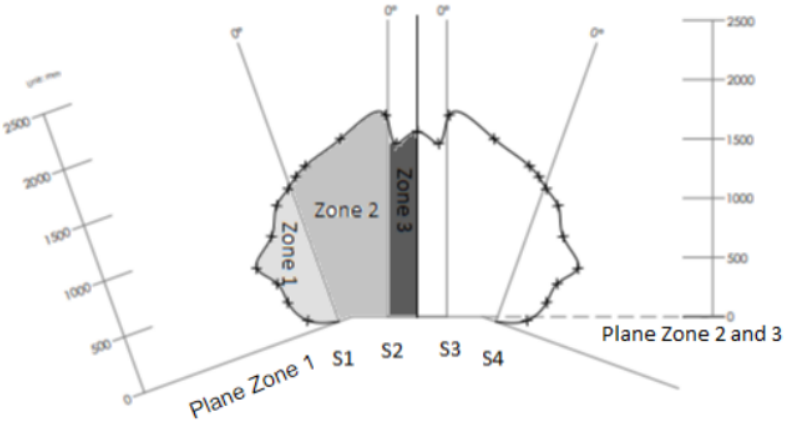

Figure 38: Whole system FoV plastic stick.

The measurements have been taken for several values of d, in the case of the metal stick, d has a range of 0-2500 mm in steps of 100 mm-200 mm, while for the plastic stick, d has a range from 0-1600 mm in steps of 100 mm-200 mm. The plastic stick range is smaller because the setup can not detect it a distance further than 1600 mm. These measurements have been taken for the three different zones that are pointed out in both Figure 37 and Figure 38. For zone 1, the reference plane for the measurements is the one of sensor 1, while for zone 2 and 3 the reference plane is the one of sensor 2. All the sensors Bus COMM signal have been watched at the same time since in zones between sensors, it would be possible that a sensor can receive a cross echo and not its direct echo. The right half plane has been replicated, assuming the ideality of the sensors.

Table 4: Metal stick whole FoV measurements.

Zone 1		Zone 2		Zone 3	
X (cm)	d (cm)	X (cm)	d (cm)	X (cm)	d (cm)
-44	15	-13	262	5	272
-60	30	-37	236	25	285
-79	47	-46	221	45	270
-88	66	-54	200		
-92	82	-74	175		
-96	100	-110	163		
-114	120	-139	145		
-96	133				
-82	152				
-55	170				
-40	180				
-21	200				
-10	215				

Table 5: Plastic stick whole FoV measurements.

Zone 1		Zone 2		Zone 3	
X (cm)	d (cm)	X (cm)	d (cm)	X (cm)	d (cm)
-24.5	10	-2	170	5	272
-35	30	-27	150	45	285
-38	48	-40	130	25	270
-50	66	-78	120		
-29	87	-105	101		
-16	110				
-2	120				

4.6 Real Time Distance Measurement

4.6.1 Hardware Preparation

Due to Arduino Uno Rev3 is not able to read voltages higher than 5V through its analog pins, and the COMM Bus signal assumes a range of values from 8.5V to 1V. For that reason, a voltage divider is used to make sure that the input of analog Arduino pin is not higer than 5V. In this way, it is possible to reduce the voltage by a factor that will depend on the resistances chosen for the formula (4)[37].

$$V_0 = \frac{R_2}{R_2 + R_1} V_{in} \tag{4}$$

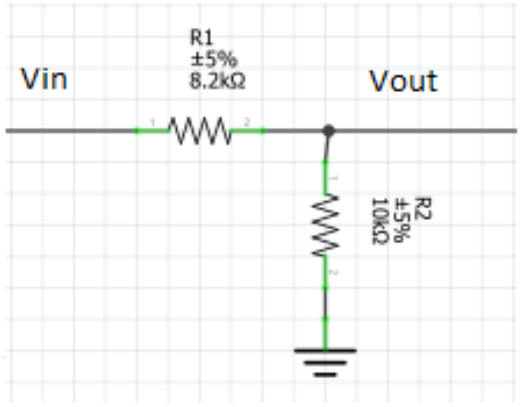

Figure 39: Voltage divider schematic.

It has been decided to choose R1 = 8.2KΩ and R2 = 10KΩ as the values of the voltage divider resistors. These resistor values are chosen since for the maximum value of the input signal, in this case 8V, output voltage would be close to 5V which is what is interesting because with other values of resistances the range of V_{out} could be smaller being thus more difficult the detection of the different pulses. Note that, others couple of resistor would fix here as long as these obey the equation. V_{in} corresponds to the COMM Bus signal of each sensor and V_{out} corresponds to the same value as V_{in} but reduced by a factor

[37] Krzentz, S. V.: Voltage divider (1998)

of 0.55. Therefore, the new range of values is 4.7V-0.55V. Now, Arduino is already able to read the input signal of its analog pins. The following figure shows the Arduino schematic (Figure 40).

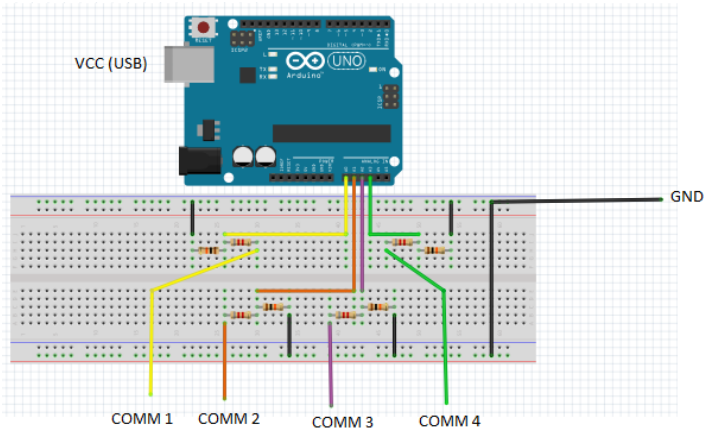

Figure 40: Arduino connexions.

4.6.2 Software Operation

The software developed calculates the distance between each of the setup sensors to an object in real time, exactly showing the distance each period T of the COMM signal. Remark that each period T lasts approximately 250 ms. Arduino reads the COMM Bus signal from each of the sensors and processes it. It means that Arduino detects each of the different pulses, both from the ECU and from the sensor and after a sensor activation by the ECU, if Arduino detects two pulses coming from the sensor, the sent and received, it will calculate the distance in time between them by getting the timestamps of both pulses with the *micros*() function. Followed by applying the formula of section 2.3.1, Arduino returns the distance value in length units, exactly in centimeters. The *micros*() function returns the time value from when arduino is turned on until the instant in which the function is called. Besides, the software detects the cross echo but it does not calculate the distance between the sensor that has received the cross echo and the object. Note that the software measurements range goes from 19 cm to 3 m.

Below, there are a tables comparing the actual distance with the measured distance when the object is placed in a short, medium and long distance from the setup.

Table 6: Measured value for a short actual distance.

Real Distance (cm)	Measured Distance (cm)
45	45.36
45	45.50
45	42.84
45	42.70
45	45.50
45	42.84
45	45.50
45	45.64
45	45.50
45	42.84

Table 7: Measured value for a medium actual distance.

Real Distance (cm)	Measured Distance (cm)
125	125.44
125	125.58
125	125.44
125	126
125	122.78
125	125.58
125	125.44
125	128.38
125	122.78
125	125.72

Table 8: Measured value for a large actual distance.

Real Distance (cm)	Measured Distance (cm)
235	235.20
235	234.78
235	235.62
235	232.12
235	232.68
235	232.12
235	232.68
235	234.78
235	232.68
235	234.71

In the tables it is detected that for an actual distance X, the measured distance changes in a range of X+-3 cm. Besides, if the actual distance is changed just 1 cm the measured distance still being the same or jump a 3 cm step. It means that the systems now has a sensibility of 3 cm. With the purpose of fix it a diagnosis has been done and have been concluded that there are three possible cases where these errors may come from:

1.) Arduino is not enough fast to detect the change voltage signal, so that Arduino detects the sent pulse with a delay. The equation $\frac{1}{f} = T$ is used to know how much Arduino needs to take a sample. Arduino works with a f=16Mhz. It means that Arduino takes a sample from the signal each $6,25 \cdot 10^{-8}$s. If the error of the distance measured is 3 cm, maybe Arduino has a delay detecting the received pulse. Applying the equation of section 2.3.1 is known that this 3 cm in time are 0.1765 ms (where ν=340 m/s). Therefore, if Arduino takes a sample every $6,25 \cdot 10^{-8}$s, it will take more than one sample in 0.1765 ms. For that reason, Arduino is enough fast and the measurement problem does not come from it[38].

2.) The pulse that corresponds to the direct echo hides information in its width. The duration of the pulse is measured for different types of objects but the same width result is always obtained, 3.9 ms. Accordingly with the result obtained,the measurement problem does not come from it either.

3.) The direct echo received by the sensor comes from different points where the signal has bounced. Depends on the signal bounced, the distance change its the value. The distance is calculated from more than one period T without moving the object position and the same distance is obtained always.

With the aim of solving this error in the measurements, it is calculated the arithmetic mean of the different values in order to stabilize the final result (5). Consequently, now a final measurement is acquired depending on the selected mean whereas previously a final measurement was obtained for each period T of the COMM signal. The number of period T per final result is equal to N[39].

$$Mean(X) = \bar{x} = \frac{\sum_{i=1}^{N} X_i}{N} \tag{5}$$

[38] Frequency and Period Time relation.
[39] Arithmetic Mean Formula.

N has value of 400, 200, 100, 50 and 20 assigned, for long to short distances. In the section 6, results that have been obtained for each N are shown. Note that for each of both N value and kind of distance(long, medium or short) has been taken ten samples.

In the results shown, it is observed that the distance from the sensor to the object is not a variable to taken into account. Also, the final measurements are stabilized in all cases, but logically, a greater stabilization can be seen for the N values of 400 and 200. Finally, the N value chosen for the distance calculation is N=20. Since for a greater N, too much time is needed by Arduino to show the final measurement and this is not of interest for parking system.

Once the N value is chosen, the software is implemented in order to not calculate the distance between an object to a sensor, but the one between object and bumper. For this implementation, the objects are divided into two groups, large and small. It is assumed that an object is cataloged as large when 3 or more sensors are detecting it, whereas when only two sensors detect it, it is classified as small. When a large object is detected, the minimum distance between sensor and object will be shown, since it will be the same distance between object and bumper Figure 41. While when a small object is detected, the trigonometric relationship of section 2.3.2 will be applied to calculate the distance between the object and the bumper. In case only one sensor detects an object, the distance shown is the one that goes from the sensor to the object.

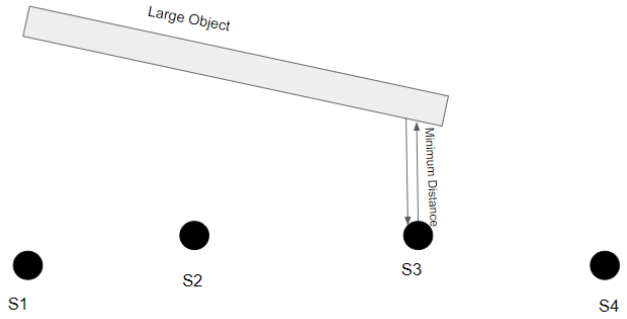

Figure 41: Example of a large object situation.

4.6.3 Sensitivity Measurement

This experiment consists of determining the sensitivity of the setup. Note that, with setting the sensitivy of the system you also set the accuracy accordingly and it will be implemented in the environment simulation. As software initial condicions for this experiment it does not contain the last part implemented about the distance from the bumper to an object. Besides, the N value set is 400, since now the delay in obtaining the final measurement does not matter and it is useful to have a result as stable as possible.

The procedure consists of placing an object at a X distance and take the result measured by Arduino. Followed by moving the setup 2 mm away from it, this is possible thanks to the rotating mechanism that the moveable platform of the setup has. Once the 2 mm are moved, the result are recalculated by Arduino. The process is repeated in steps of 2 mm until the measurement obtained by Arduino has changed to the next measurement step. Depends on this step, the sensitivity of the system based on the actual measurement is determinated. Finally it is viewed that when is changed 1 cm from the actual distance, the next measured step changes 1 cm as well.

This process has been repeated for long, medium and short distances and the results obtained are in the following Table 9, Table 10 and Table 11:

Table 9: Short distance sensitivity experiment results.

Actual Distance (cm)	Measured Distance (cm)
44.8	43.61
45	43.63
45.2	43.93
45.4	44.07
45.6	44.73
45.8	44.89
46	45.43

Table 10: Medium distance sensitivity experiment results.

Actual Distance (cm)	Measured Distance (cm)
112.8	111.95
113	112.17
113.2	112.31
113.4	112.45
113.6	112.72
113.8	112.87
114	113.11

Table 11: Long distance sensitivity experiment results.

Actual Distance (cm)	Measured Distance (cm)
224.8	223.92
225	224.36
225.2	224.65
225.4	224.70
225.6	224.96
225.8	225.26
226	225.28

Due to the volatility for units smaller than the centimeters, it is decided to establish 1 cm as the sensitivity of the system. Note that the results obtained will be always one centimeter less than the actual distance.

5 Conclusions

Once the methodology was followed and the different experiments were elaborated, the results that were obtained, will be discussed below.

Regarding the field of view (FoV) determination experiment, it should be noted that the experiment has been carried out with three different objects, in particular: a round shaped metal stick, a round shaped plastic stick and a square shaped metal stick. In addition, it was experimented with a square shaped wooden stick, but the experiment could not be validated for the reason that its thickness was considerable and the FoV could not be determined with accuracy. Once obtained the results with the different point objects, it has been concluded that the material does not affect the FoV determination, but the form alters the result seeing that for a square shape better results have been obtained. This is because the echo of the signal sent by the sensor is easier to receive when it bounces on a square object than a round one. The results achieved are the following: a horizontal FoV of 60 degrees and vertical around about 30 degrees and a maximum length of 2.6 m as well. About the FoV width , the results have been similar to what was expected, while the FoV length has been better than expected in previous studies.

With respect to the experiment of maximum and minimum length, it has been viewed that the Bosch sensor is able to detect objects at a distance of 4 meters, but is not very reliable since at these distances it is not able to detect the object at 100% of the time. Therefore, to achieve 100% effectiveness, the maximum distance detectable by the sensor is reduced to 3.6m. Note that in this experiment a greater maximum length has been obtained than in the FoV experiment because in this experiment the setup has been placed in front of a wall and not a point object, so that the wall is easier to detect due to its size.

On the other hand it has also been demonstrated if these sensors have implemented the cross echo detection. The cross echo is the signal that comes from another sensor after it has bounced on an object. During the experiments, its operation has been confirmed, in such a way that with the cross echo functionality implemented, the whole sensor setup FoV improves.

Finally, the calculation of the distance between object and sensor has been tested in such a way that the result obtained was as accurate as possible. This has been achieved without any problem reading the communication signal between sensor and control unit. Later, the script implementation for Arduino was carried out, which was able to calculate the distance to an object in real time without having to observe the communication Bus signal. Initially, the results obtained had an measurement failure about 3 cm with respect to the actual measurement approximately, even though this failure was not always obtained in the measurement. To solve this error in the measurement, it has been proposed to calculate the average of N results to get a mean value measured and thus improve the measure accuracy, reaching a maximum error of 1 cm. This mean calculation implementation is used to get a better sensitivity as well.

To sum up, remark that the Bosch sensors are very powerful which is not reflected in the user-level functionality. It is because a parking assistance system does not require this accuracy and these wide ranges of vision. On the other hand, a system for autonomous driving need it, and according to the results obtained, Bosch sensors are good to do it. Emphasize that all the information or results collected

during the experiments are good enough to create a simulation environment for valet parking use cases that contribute to autonomous driving.

As aspects to improve, results more reliable could have been obtained if the sensors had been installed in the car. Since in the test setup an attempt has been made to imitate Honda's bumper in terms of distance between sensors, both vertical and horizontal, but the exact sensor orientation could not be replicated.

Finally, the work to be carried out in the future could be to develop dynamic tests, possibly with the sensors in the car, since the experiments have been run in static. The information of which could be implemented to improve the simulation environment.

```
distance middle-left sensor:
59.99
distance middle-left sensor:
60.13
distance middle-left sensor:
61.19
distance middle-left sensor:
60.25
distance middle-left sensor:
60.28
distance middle-left sensor:
59.98
distance middle-left sensor:
60.53
distance middle-left sensor:
60.12
distance middle-left sensor:
61.73
distance middle-left sensor:
60.51
```

Figure 42: Samples medium distance and N=20.

```
distance middle-left sensor:
112.25
distance middle-left sensor:
112.24
distance middle-left sensor:
112.10
distance middle-left sensor:
112.36
distance middle-left sensor:
112.23
distance middle-left sensor:
112.24
distance middle-left sensor:
112.13
distance middle-left sensor:
112.13
distance middle-left sensor:
112.10
distance middle-left sensor:
112.12
```

Figure 43: Samples medium distance and N=20.

```
distance middle-left sensor:
219.95
distance middle-left sensor:
219.27
distance middle-left sensor:
219.79
distance middle-left sensor:
219.51
distance middle-left sensor:
219.53
distance middle-left sensor:
219.69
distance middle-left sensor:
219.66
distance middle-left sensor:
219.92
distance middle-left sensor:
220.25
distance middle-left sensor:
219.55
```

Figure 44: Samples large distance and N=20.

```
distance middle-left sensor:
60.51
distance middle-left sensor:
59.97
distance middle-left sensor:
60.24
distance middle-left sensor:
60.87
distance middle-left sensor:
60.40
distance middle-left sensor:
60.45
distance middle-left sensor:
61.41
distance middle-left sensor:
60.34
distance middle-left sensor:
60.34
distance middle-left sensor:
60.56
```

Figure 45: Samples in a short distance and N=50.

```
distance middle-left sensor:
112.05
distance middle-left sensor:
112.21
distance middle-left sensor:
112.39
distance middle-left sensor:
112.15
distance middle-left sensor:
112.17
distance middle-left sensor:
112.17
distance middle-left sensor:
112.21
distance middle-left sensor:
112.12
distance middle-left sensor:
112.11
distance middle-left sensor:
112.22
```

Figure 46: Samples in a medium distance and N=50.

```
distance middle-left sensor:
219.39
distance middle-left sensor:
219.91
distance middle-left sensor:
219.70
distance middle-left sensor:
220.02
distance middle-left sensor:
219.73
distance middle-left sensor:
219.69
distance middle-left sensor:
219.69
distance middle-left sensor:
219.71
distance middle-left sensor:
219.97
distance middle-left sensor:
219.91
```

Figure 47: Samples in a large distance and N=50.

```
distance middle-left sensor:
60.34
distance middle-left sensor:
60.44
distance middle-left sensor:
60.55
distance middle-left sensor:
60.10
distance middle-left sensor:
60.58
distance middle-left sensor:
60.15
distance middle-left sensor:
60.37
distance middle-left sensor:
60.50
distance middle-left sensor:
60.77
distance middle-left sensor:
60.48
```

Figure 48: Samples in a short distance and N=100.

```
distance middle-left sensor:
112.22
distance middle-left sensor:
112.09
distance middle-left sensor:
112.17
distance middle-left sensor:
112.17
distance middle-left sensor:
112.22
distance middle-left sensor:
112.24
distance middle-left sensor:
112.16
distance middle-left sensor:
112.20
distance middle-left sensor:
112.46
distance middle-left sensor:
112.20
```

Figure 49: Samples in a medium distance and N=100.

```
distance middle-left sensor:
220.10
distance middle-left sensor:
219.91
distance middle-left sensor:
219.82
distance middle-left sensor:
219.97
distance middle-left sensor:
219.80
distance middle-left sensor:
220.20
distance middle-left sensor:
219.99
distance middle-left sensor:
219.79
distance middle-left sensor:
219.82
distance middle-left sensor:
219.94
```

Figure 50: Samples in a large distance and N=100.

```
distance middle-left sensor:
60.31
distance middle-left sensor:
60.58
distance middle-left sensor:
60.44
distance middle-left sensor:
60.45
distance middle-left sensor:
60.17
distance middle-left sensor:
60.52
distance middle-left sensor:
60.58
distance middle-left sensor:
60.33
distance middle-left sensor:
60.39
distance middle-left sensor:
60.52
```

Figure 51: Samples in a short distance and N=200.

```
distance middle-left sensor:
112.18
distance middle-left sensor:
112.24
distance middle-left sensor:
112.17
distance middle-left sensor:
112.18
distance middle-left sensor:
112.24
distance middle-left sensor:
112.14
distance middle-left sensor:
112.18
distance middle-left sensor:
112.15
distance middle-left sensor:
112.25
distance middle-left sensor:
112.19
```

Figure 52: Samples in a medium distance and N=200.

```
distance middle-left sensor:
219.83
distance middle-left sensor:
219.96
distance middle-left sensor:
219.96
distance middle-left sensor:
218.85
distance middle-left sensor:
219.95
distance middle-left sensor:
219.78
distance middle-left sensor:
219.95
distance middle-left sensor:
219.86
distance middle-left sensor:
219.98
distance middle-left sensor:
218.79
```

Figure 53: Samples in a large distance and N=200.

```
distance middle-left sensor:
60.30
distance middle-left sensor:
60.25
distance middle-left sensor:
60.53
distance middle-left sensor:
60.39
distance middle-left sensor:
60.74
distance middle-left sensor:
60.27
distance middle-left sensor:
60.63
distance middle-left sensor:
60.40
distance middle-left sensor:
60.35
distance middle-left sensor:
60.37
```

Figure 54: Samples in a short distance and N=400.

```
distance middle-left sensor:
112.18
distance middle-left sensor:
112.16
distance middle-left sensor:
112.16
distance middle-left sensor:
112.16
distance middle-left sensor:
112.20
distance middle-left sensor:
112.18
distance middle-left sensor:
112.17
distance middle-left sensor:
112.17
distance middle-left sensor:
112.18
distance middle-left sensor:
112.19
```

Figure 55: Samples in a medium distance and N=400.

```
distance middle-left sensor:
219.95
distance middle-left sensor:
219.78
distance middle-left sensor:
219.94
distance middle-left sensor:
219.85
distance middle-left sensor:
219.95
distance middle-left sensor:
219.84
distance middle-left sensor:
219.86
distance middle-left sensor:
220.23
distance middle-left sensor:
220.00
distance middle-left sensor:
219.90
```

Figure 56: Samples in a large distance and N=400.

References

Arduino IDE. Arduino IDE. URL: https://www.arduino.cc/en/Main/Software.

Arduino UNO Rev3. Arduino UNO Rev3 Tech Specs. URL: https://store.arduino.cc/arduino-uno-rev3.

Arithmetic Mean Formula. URL: https://en.wikipedia.org/wiki/Arithmetic_mean.

Bosch Operating Intructions. Bosch operating intructions. 2009.

Bosch Ultrasonic Sensor. URL: https://www.bosch-mobility-solutions.com/en/products-and-services/passenger-cars-and-light-commercial-vehicles/driver-assistance-systems/construction-zone-assist/ultrasonic-sensor/.

Carullo, A. et al.: Ultrasonic sensor distance measurement (2001)
Carullo, Alessio; Parvis, Marco: Ultrasonic sensor for distance measurement in automotive applications, in: IEEE Sensors journal, 1, p. 143, (2001)

Data acquisition. Data acquisition. URL: https://www.ni.com/data-acquisition/d/.

Frequency and Period Time relation. URL: https://en.wikipedia.org/wiki/Frequency.

Fu, J.: Diss., Ultrasonic sensor model (2018)
Fu, Junfeng: Auswahl und Implementation eines Ultraschall-Sensormodells für die Fahrzeuganwendung, (2018)

Fu, J. et al.: Diss., Setup for ultrasonic models validation (2017)
Fu, Junfeng; She, Jiahao; Shen, Liwen; Wanf, Qin,; Zuo, Yueyao: Aufbau eines geeigneten Test-Setups zur Validierung von Ultraschallsensor-Modellen, (2017)

Jaffe, B.: Piezoelectric ceramics (2012)
Jaffe, Bernard: Piezoelectric ceramics, Elsevier, (2012)

Kishonti, L.: Real and simulated tests (2017)
Kishonti, László: In autonomous driving, real-world testing is taking a backseat, (2017)

Krzentz, S. V.: Voltage divider (1998)
Krzentz, Steven V: Resistance voltage divider circuit, Google Patents, (1998)

Nakamura, K.: Ultrasonic applications (2012)
Nakamura, Kentaro: Ultrasonic Transducers: Materials and Design for Sensors, Actuators and medical applications, Elsevier, (2012)

Navarro: Ultrasonic distance measurement (2004)
Navarro: Sensores de Ultrasonido usados en Robótica Móvil para la Medición de Distancias, in: Scientia et Technica, 273, (2004)

Olympus, N.: Ultrasonic Transducers (2006)
Olympus, NDT: Ultrasonic transducers technical notes, in: Technical brochure: Olympus NDT, Waltham, MA, pp. 40–50, (2006)

Real and Simulation car tests. URL: https://mashable.com/2017/07/14/autonomous-driving-real-cars-simulations/?europe=true#FSNdrl0XsgqS.

Rubio, C.: Ultrasonic transducer (2010)
Rubio, Carlos: Fabricación de Transductores Ultrasónicos para Equipos automatizados de inspección de líneas de Tuberías, (2010)

Rubio, C.: Diss., Ultrasonic transducer for automated sytems (2018)
Rubio, Carlos: Transductores Ultrasónicos para Equipos automatizados, (2018)

Winner, H.: Handbook of Driver Assistance Systems (2014)
Winner, Hermann: Handbook of Driver Assistance Systems, ISBN: 978-3-319-09840-1, (2014)

Yang, C. E.: Piezo electric effect (2016)
Yang, Carmen Emily: What is the piezo electric effect?, (2016)